14th Australasian Fluid Mechanics Conference
Adelaide University, Adelaide, Australia
10-14 December 2001

Experiments on Natural Convection Boundary Layers -The Role of Instabilities

John C. Patterson

School of Engineering
James Cook University
Townsville, QLD, 4810 AUSTRALIA

Abstract

In this paper, an experimental investigation of the transient behaviour of the flow adjacent to a suddenly heated vertical wall is described. The experiments confirm that the primary deviation from one dimensional to two dimensional flow at a particular location occurs at the time at which the fastest travelling wave arising from the perturbation caused at startup reaches that location. Further, a secondary instability is identified which simultaneously occurs along the full length of the boundary layer and, in some locations along the plate, evidently triggers a deviation ahead of the arrival of the fastest travelling wave.

Introduction

Fluid flows that are driven by density differences are an ubiquitous part of our lives. Flows that range from the smallest scales of turbulence of a few millimetres to geophysical scales of many kilometres arise from differences in temperature, salinity or some other dissolved quantity which influences the fluid density, or perhaps from a change of phase of the fluid. The transport of the quantity which influences density is referred to as convection, and since the convection is itself the result of a gradient in the quantity, it is usually known as natural or free convection.

The applications are many; heat transfer in buildings, industrial processes, atmospheric and other geophysical flows, and heat exchangers are a few immediately recognizable examples. The variability amongst these flows is vast, with the widest possible range of length and time scales, complex geometries, difficult fluids, and a range of forcing mechanisms. However, much of the impetus for research in the area has come from a relatively few areas, including, for example, heat transfer in industrial processes and especially the role of heat exchangers, and geophysical flows.

One of the classical flows with particular relvance to the first of these applications is the seemingly relatively simple problem of the mass and heat transfer in a rectangular container subjected to a lateral temperature gradient. Originally posed in the 1950's as a problem in heat transfer through double glazed windows (Batchelor [1]) this problem is relevant to many industrial processes in which the process is somehow encased by a cooling fluid. In some cases the heat exchanger may be open to a much larger environment, in which case it is only the flow adjacent to the heated wall which is of relevance. If the fluid is pumped or somehow otherwise forced to flow the problem is no longer driven solely by the density gradient and is therefore no longer solely natural convection. These applications are not relevant to the present paper.

Even in this seemingly simple configuration, there are many complications. In may cases, the way in which the temperature gradient is applied varies with time, in some cases instantaneously, and the transient repsonse of the fluid is of interest. Further, the flows are not always laminar, and the transition to turbulence and the influence that the transition has on the heat transfer properties is also relevant. The fluids are not always simple, and the initial state of the fluid could be stratified, non stationary or otherwise difficult to deal with.

Nevertheless, significant progress has been made on the analysis of this classical problem. A great deal of literature exists for examination of the steady state flows resulting from this forcing, but it was not until 1980 (Patterson and Imberger [2]) that a detailed examination of the startup flow following the sudden heating and cooling of the vertical walls was carried out. Since then, a substantial body of knowledge describing various aspects of the startup flow and the transition to steady state has been established (see eg. [3] - [14]).

One aspect of the flow development which is central to the early transient behaviour is the development of the thermal boundary layers on the heated or cooled walls. In particular, the mechanism for the transition to two dimensional flow and the time at which that transition occurs govern the early properties of the flow. In this paper, the presence of instabilities on the boundary layer is shown from experiments to support a theory which predicts the transition time, and to provide an alternative mechanism for transition.

Background and Identification of the Role of Instabilities

The idealised problem considered here is a rectangular cavity with two opposing vertical walls heated and cooled by the same amount respectively. The resulting flow consists of rising and falling boundary layers on those walls, exiting into the central part of the cavity as heated or cooled intrusions along the ceiling and floor. These intrusions interact with the opposing wall boundary layers, with the core region of the cavity and with their source vertical boundary layers to ultimately fill the cavity with heated and cooled fluid, leaving at steady state a stratified interior region bounded by narrow vertical layers and narrow horizontal intrusions. The flow is governed by the aspect ratio of the cavity A, the Rayleigh number Ra, and the Prandtl number of the fluid Pr, where

$$A = \frac{h}{\ell} \tag{1}$$

$$Ra = \frac{g\alpha\Delta T h^3}{\nu\kappa} \tag{2}$$

$$Pr = \frac{\nu}{\kappa} \tag{3}$$

and h and ℓ are the height and length of the cavity respectively, g the acceleration due to gravity, α, ν and κ the

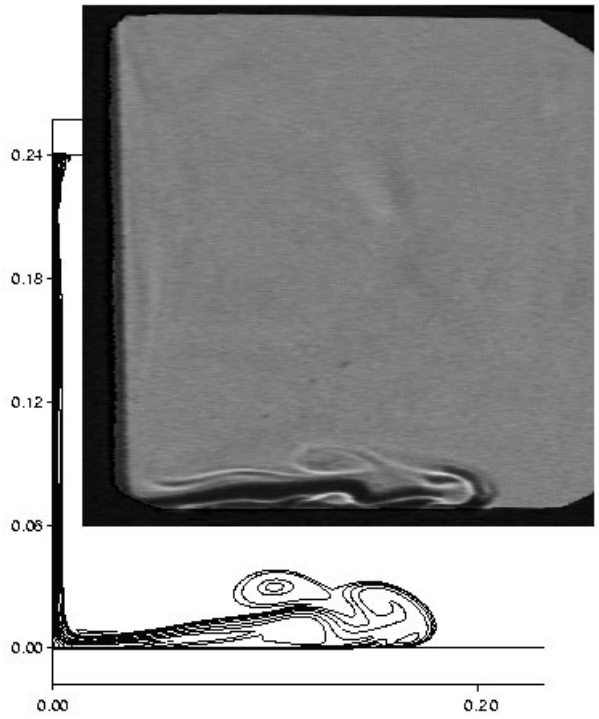

Figure 1: Numerically generated isotherms and a shadowgraph image of the cold wall boundary layer and the cold intrusion at time 43.6 sec. In this case the wall temperature difference was 16.6°C. The axis units are m. The corresponding Rayleigh number is 3.65×10^9. Note that the isotherm plot is offset to the left.

coefficient of thermal expansion, the kinematic viscosity and the thermal diffusivity of the fluid respectively and ΔT the temperature difference between each wall and the core ambient temperature.

Figure 1 shows both a shadowgraph image and a numerically generated set of temperature contours for the flow from the cold wall at an early time in the development of the flow. In this case, the cold wall is the vertical line to the left. A corresponding vertical boundary layer and hot intrusion will be present on the opposing wall and the ceiling. The temperature contours show the vertical boundary layer formed on the wall depicted as closely packed isotherms parallel to the wall (not easily visible in this shadowgraph image which was configured to optimise the visualisation of the intrusion), and a complex intrusion flow, with many small structures, particularly on the nose of the intrusion, visible in both numerical and observed images. These small structures are of interest, but are not the focus of this paper. A closer inspection of the boundary layer however does show the features which are discussed here.

Thermal Boundary Layer Development

The flow adjacent to the vertical heated and cooled walls has been shown to be closely described by the flow on a semi-infinte suddenly heated (or cooled) wall with the exception of the region near the upper boundary, where the flow is turned into the core region of the cavity (Patterson and Armfield [3]). This has been described qualitatively in the following terms (Siegal [15]). At any fixed position downstream of the end of the wall (the leading edge) the flow behaves initially as though the plate were doubly infinite, and the classical unsteady one-dimensional flow and temperature fields first described by Illingworth [16] and, in a more general context, Goldstein and Briggs [17] are appropriate. At some later time which depends on the distance from the leading edge, the flow becomes two-dimensional and steady, and is described by the solution given by Ostrach [18]. This transition from unsteady one-dimensional flow to steady two-dimensional flow occurs over a non zero time period, and travels downstream at some velocity which is determined by the parameters of the problem. The transition phase, referred to as the 'leading edge effect' (LEE), is characterised by the presence of an oscillatory component, the amplitude of which is also determined by the parameters of the problem and the location, with the oscillations growing in amplitude with increasing downstream position. According to this description therefore, a time series of temperature taken at any given point in the boundary layer will initially follow the complementary error function growth given by the one-dimensional conduction solution referred to above and given by equation (7) below, developing into a transition period which will include an oscillatory component, followed by an approximately constant value given by the steady state solution given by [18].

These phases of the flow development are clearly shown in figure 2, which shows a typical temperature time series in water, taken in the heated boundary layer 8.75 cm downstream from the leading edge, 2.70 mm in from the wall and with an imposed temperature difference of 1.17°C. The ambient temperature in this case was 34.24°C. Also shown in this figure is the theoretical solution for the one-dimensional case, given by equation (7) below.

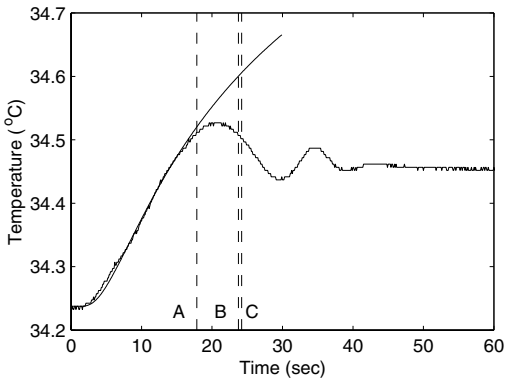

Figure 2: A typical temperature time series in the boundary layer; the parameter values for this case are given in the text. The corresponding one-dimensional solution, given by equation (7), is overlaid. The meaning of the three broken vertical lines marked A, B, and C is given in the text.

According to the description of the flow development, the early part of the boundary layer flow is described by the one dimensional solution for the suddenly heated doubly infinite plate, and figure 2 clearly shows that, for times less than approximately 15 s, the two are virtually coincident. The deviation of the experimental result from the one dimensional solution after that time implies that the LEE has arrived at this location, supported by the following oscillatory component which decays into a steady state as predicted. The time taken for the flow near the

boundary to reach steady state is therefore largely controlled by the timing of these events, and an understanding of these processes is therefore of some interest.

Evidently the deviation from the one dimensional solution at a particular location occurs when a signal from the leading edge arrives at that location. Both Goldstein and Briggs [17] and Brown and Riley [19] obtained estimates for the arrival times, based on the assumption that the signal was advected by the main flow. Their estimates were, respectively,

$$y_p(\tau) = max \int_0^\tau v(x,t)dt, \tag{4}$$

and

$$y_p(\tau) = \int_0^\tau max[v(x,t)]dt, \tag{5}$$

where y_p is the distance the LEE penetrates in time τ, and $v(x,t)$ is the boundary layer velocity given by equation (6) below.

The results of inverting these expressions to find the times of arrival at 8.75 cm in the case shown in figure 2 are shown as the vertical lines marked B and C on the figure. The values predicted are similar, approximately 24 s, but are both considerably later than the observed deviation, at around 15 s. This result is consistent with the constant flux experiments described in Gebhart and Mahajan [12], Joshi and Gebhart [13], and Gebhart *et al.* [14], and the isothermal numerical and experimental results of Schladow [5], Armfield and Patterson [4] and Schöpf and Patterson [6], all of which showed that the LEE arrived significantly earlier than the times predicted by the simple advection theory.

A different estimate of the arrival time of the LEE was provided by Armfield and Patterson [4]. Their prediction was based on the speed of the fastest of the travelling waves generated on the one-dimensional boundary layer by the initial perturbation caused by the start up. This required an analysis of the stability properties of the boundary layer to calculate the speed of the fastest wave, and the amplification spectrum to establish the properties of the following waves. Numerical simulations of the cavity flow appeared to strongly support these ideas. Subsequent papers along these lines included theoretical analyses by Daniels and Patterson [10, 11], numerical investigations by Brooker and co-workers [8, 9] and a number of experimental investigations (Schöpf and Patterson [6], Graham and Patterson [20] and Patterson *et al.* [21]).

A separate effect was also apparent in the experimental results of Joshi and Gebhart [13] for the isoflux heating case. Here, at high heating rates, a deviation from the one-dimensional solution apparently appeared at all locations simultaneously, ahead of the passage of the LEE. The same effect was evident, though not discussed, in the experimental results for the isothermal case given by Graham and Patterson [20]. This observation had not been noted previously in numerical investigations for either the isoflux or isothermal heating cases [2, 4, 22, 23]. This suggested that the instability was convective in nature, with the small perturbations inherent in the numerical solution simply not amplifying sufficiently to be visible before being carried away by the flow. On the other hand, the natural disturbances necessarily present in an experiment may be sufficiently large to become visible.

Brooker *et al.* [9] was however able to observe this secondary instability in numerical simulations. In this paper, a numerical simulation of the side heated cavity was subjected to random perturbations in temperature along the length of the heated wall for a particular set of parameter values; after a certain time, the temperature time series at the downstream end of the boundary layer showed evidence of the presence of a significant deviation from the one dimensional solution, well ahead of the arrival of the LEE, similar to the results described above from experiments.

As noted, some experimental data [20, 21] also clearly demonstrates the presence of this effect, as shown in figure 3. The time series from the two lowest placed thermistor at least qualitatively show the expected behaviour, but the time series from the upper two definitely do not, with deviation from the expected one-dimensional signal much earlier than predicted, and an oscillatory behaviour quite different to that evident at the upstream end.

The perturbed numerical simulations in [9] were compared with similar experimental data for the same parameter values and, by adjusting the amplitude of the numerical perturbations, were shown to match well; by using direct stability analysis these deviations were shown to be also the result of an instability on the boundary layer.

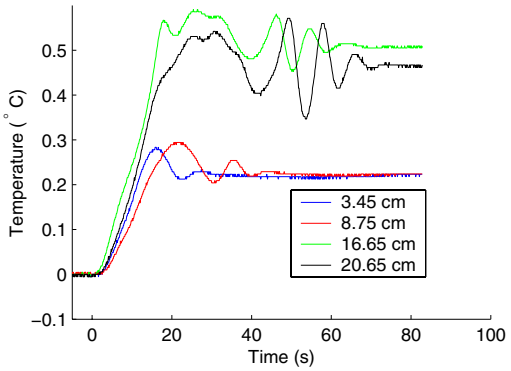

Figure 3: Temperature time series in the boundary layer taken at the heights shown on the figure, for the same parameter set used in figure 2.

Leading Edge Effect

As noted above, the speed of the LEE was initially modelled as though the signal was being carried by the main flow in the boundary layer. The penetration distance of the LEE was modelled by equations (4) and (5) above from [17] and [19] respectively. In equations (4) and (5), $v(x,t)$ is the vetical velocity given by, from the solution of the one dimensional problem,

$$v_B(x,t) = \frac{4g\beta\Delta T t}{1-Pr}\left[i^2\mathrm{erfc}\left(\frac{x}{2\sqrt{\kappa t}}\right) - i^2\mathrm{erfc}\left(\frac{x}{2\sqrt{\nu t}}\right)\right]. \tag{6}$$

The corresponding temperature is

$$T_B(x,t) = T_0 + \Delta T\mathrm{erfc}\left(\frac{x}{2\sqrt{\kappa t}}\right), \tag{7}$$

where, in equations (6) and (7), T_0 is the initial tem-

perature, $i^2\text{erfc}(z)$ is the second integral of the complementary error function $erfc(z)$ with argument z and the other variables are given above. The subscript B in equations (6) and (7) refers to the base flow condition for the subsequent stability analysis.

The model proposed in [4] was based on the principle that the fastest travelling wave from the perturbation introduced at the leading edge by the start up was responsible for triggering the transition to two dimensional flow, and therefore was a measure of the arrival of the leading edge effect. Daniels and Patterson [10] showed that these waves always travelled at a velocity higher than the fastest advective velocity in the boundary layer, which implied that the leading edge signal would arrive sooner than predicted by boundary layer velocity based models.

The penetration distance $y_p(\tau)$ of the LEE at time τ, following this model, is then given by

$$y_p(\tau) = \int_0^\tau c_{r\,max}(t)dt, \tag{8}$$

where $c_{r\,max}$ is the maximum phase velocity at time t. To evaluate these integrals for the parameters given, the stability properties of the one-dimensional solutions in each case must first be determined. The formulation and solution of the linear stability analysis has been previously addressed (see, e.g. [4, 10]) and only a brief description is given here.

The one-dimensional solutions given by equations (6) and (7) are referred to as the base flow. To determine the stability properties of the base flow, it is modified by a small perturbation of the form

$$\Psi = \psi_B + \epsilon Re\left[\psi(x)e^{i\alpha(y-c\tilde{t})}\right] \tag{9}$$

and

$$\Theta = T_B + \epsilon Re\left[\theta(x)e^{i\alpha(y-c\tilde{t})}\right], \tag{10}$$

where ϵ is a small parameter; Re signifies the real part of the following expression; Ψ and ψ are total and perturbation stream functions respectively, defined in the usual way; Θ and θ are total and perturbation temperatures respectively; and the subscript B refers to the base flow values. Since travelling waves are sought, the wavenumber α is real, and c is complex with real part c_r and imaginary part c_i; c_r is the wave phase speed, and αc_i is the amplification. Here $\tilde{t}$ is the time associated with the waves; t associated with the base flow is only a parameter in the following stability analysis. This is consistent with assuming that any variations with respect to the waves are on a much faster time scale than the variations associated with the growth of the base flow [10]. In other words, the stability calculations are carried out at a particular time as though the base flow velocity and temperature fields were fixed at that time.

When Ψ and Θ are inserted in the equations of motion, the base flow terms cancelled, and the result linearised with respect to ϵ, a sixth order ordinary differential equation system for the eigenfunctions ψ and θ, with eigenvalues α, c_r and c_i, arises. The solution of these equations has been described in [4] and [10] and will not be discussed further here.

To evaluate the time taken for the leading edge effect to reach a given position following this model, the maximum wave speed is required as a function of time. Thus a large number of evaluations of the wave speed spectra are required to allow an integration over time of the maximum wave speed. Again, the details of these calculations are omitted here. It is worth noting however the following features: first, at large times, the wave speed spectrum with respect to wave number is highly peaked, with a clear maximum; second, at large times, the maximum wave speed is at a wavenumber which is not amplified, although a significant part of the spectrum is amplified; third, as time decreases, the maximum is less well defined with a much flatter distribution; fourth, the eigenvalues become increasingly difficult to find as time decreases, which may be related to the observation that the amplified part of the spectrum is increasingly difficult to locate; and finally, apart from the time near zero, the maximum wave velocity is evidently a linear function of time.

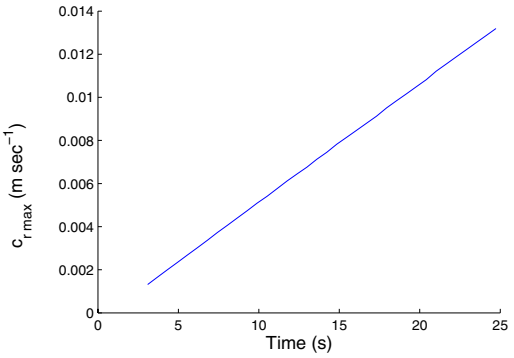

Figure 4: Maximum phase velocity $c_{r_{max}}$ as a function of time for the experimantal case discussed in the text.

The result for the parameter set introduced above is shown in figure 4. As noted, values for $c_{r_{max}}$ became increasingly difficult to find near $t = 0$, and solutions could not be found for $t < 3.1$ s. The dependence is however clearly linear, with a slope of 0.549×10^{-3} ms^{-1}, and an extrapolation of the data gives that $c_{r_{max}} = 0$ at $t = 0.66$ s. It is therefore assumed that the velocity is zero for $t < 0.66$ s giving a simple inversion to calculate the time required to reach a given y location.

For the case shown in figure 2, the time calculated in this way to reach the thermistor location at 8.75 cm is 17.84 s, shown on figure 2 as the vertical broken line marked A. Qualitatively at least, this estimate is a very good indicator of the time at which the response deviates from the one-dimensional solution.

The temperature time series results shown in figures 2 and 3 arose from an experimental investigation of the phenomena [21]. The experiments utilised a rig which has been developed for unsteady natural convection experiments, and the procedures have been reported widely (see eg., [3, 6, 7]). Briefly, the working fluid is contained between two vertical 1.15 mm thick copper plates, with the upper and lower and remaining vertical walls constructed from 1.5 cm thick perspex. The copper plates are separated from hot and cold water baths at each end by an air gap, with the heated and cooled water restrained by removable, pnuematically operated gates. The air gaps are maintained at the working temperature T_0, and the hot and cold baths at temperatures $T_0 \pm \Delta T$ respectively. At initiation of the experiment, the gates are raised simultaneously, and the heated and cooled water floods against

the copper plates, providing rapid heating and cooling.

A version of this rig used for investigating the LEE used only heating on one wall, with the cold wall held at T_0. A schematic of the rig (not to scale) is shown in figure 5. Full details of the experimental procedures are given in [21].

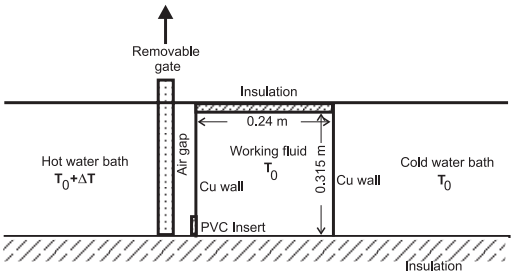

Figure 5: The experimental rig used for the LEE expperiments; the full cavity rig has cooling on the opposite side as well. The PVC insert at the bottom of the cold wall was placed to simulate the leading edge, and is not present in the full cavity experiments.

In all a total of 14 separate experiments were carried out over a range of temperature differences from 1.17°C to 8.66°C, corresponding to a range of Rayleigh numbers from 3.3×10^8 to 2.4×10^9. In each experiment, at least four time series were taken at various points along the plate, at approximately equal distances from the wall within the thermal boundary layer. The time series shown in figures 2 and 3 are typical of those taken near the upstream end of the wall. The time series further downstream were often influenced by the secondary instability described above, and will be discussed later. This limited LEE analysis to a total of 19 time series.

The time series were all qualitatively similar to that shown in figure 2. A fitting procedure (described in [21]) was used to determine the observed time of departure from the one dimensional solution. For the case shown in figure 2, the departure time was determined to be 15.36 s, considerably shorter than the estimates from equations (4) and (5). However, the time estimated from equation (8) of 17.84 sec is considerably closer. As noted, that value is shown on figure 2 as the vertical dashed line marked A.

The values of the three estimates (t_{BR} from equation (4), t_{GB} from equation (5) and t_{CR} from equation (8)) and the observed value t_{act} for each of the 19 possible time series is givne in Table 1 below, together with the ratio $\frac{t_{CR}}{t_{act}}$. In the table, y_t is the distance from the leading edge at which the measurement was taken.

Clearly, the estimate t_{CR} is a far superior estimate to either t_{GB} or t_{BR}. Although some of the estimates are poor, in general they are within 10%.

The time scale for the arrival of the travelling waves at a particular location may be obtained by approximating the stability equations. From those equations, the velocity scale for the travelling wave velocity is given by, for $Pr > 1$

$$\hat{v} \sim v_{adv}\sqrt{Pr}, \tag{11}$$

where v_{adv} is the velocity scale of vertical boundary layer velocity given by, from [2] or more directly from equation (6),

$$v_{adv} \sim \frac{g\beta\Delta T}{Pr}t, \tag{12}$$

and so the time scale for the time of arrival at position y is given by

$$\tau \sim \left(\frac{y\sqrt{Pr}}{g\beta\Delta T}\right)^{\frac{1}{2}}. \tag{13}$$

Figure 6 shows the arrival times t_{act} plotted against τ defined in equation (13). Although there is some scatter, the arrival times are approximately a linear function of τ, and a linear regression through the data gives a slope of 2.27 with $R^2 = 0.88$.

This scaling result together with the direct comparison in table 1 lends support to the conclusions reached by numerical analysis - that the speed at which the LEE travels along the plate is best given by the speed of the fastest travelling wave which results from the perturbation of the starting one-dimensional boundary layer. The time series also show the anticipated following oscillatory behaviour. It is to be expected that the period of these oscillations corresponds to the period of the maximally amplified waves travelling on the boundary layer. This is indeed the case, although those details are not discussed here (see [21]).

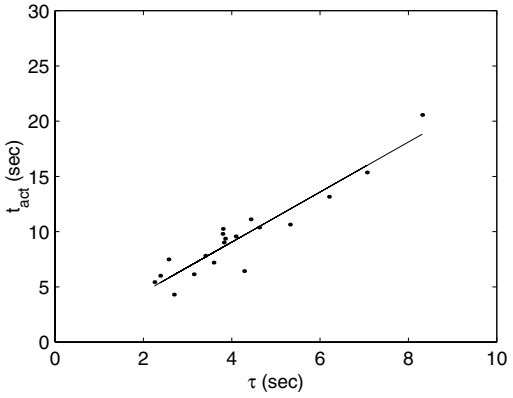

Figure 6: The time of arrival observed in the experiments t_{act} for all experiments, plotted against the scaled time τ. The solid line is the line of best fit.

Secondary Instability

The secondary instability which forms on the thermal boundary layer downstream of the travelling LEE was clearly observed in the experiments of Joshi and Gebhart [13], Graham and Patterson [20] and in more detail in Patterson *et al.* [21], and in the perturbed numerical results of Brooker *et al.* [9]. Although this last paper demonstrated the existence of the instability and documented its characteristics, the relationship to the existing experimental or detailed numerical results was not confirmed.

The stability analysis described above was based on the assumption that the time scale for development of the thermal boundary layer is long when compared with the time scales associated with the waves travelling on the boundary layer. This means that time is a parameter in the stability equations, which are solved as though the

Ra	Pr	$y_t(cm)$	$t_{BR}(sec)$	$t_{GB}(sec)$	$t_{act}(sec)$	$t_{CR}(sec)$	$\frac{t_{CR}}{t_{act}}$
1.89×10^9	5.42	3.45	7.61	7.75	5.42	5.73	1.06
$''$	$''$	8.75	12.14	12.36	7.19	9.12	1.27
1.68×10^9	5.34	3.45	8.10	8.25	6.01	6.05	1.01
$''$	$''$	8.75	12.90	13.15	10.25	9.65	0.94
1.33×10^9	5.27	3.45	9.08	9.25	4.30	6.83	1.59
$''$	$''$	8.75	14.46	14.74	6.43	10.87	1.69
1.47×10^9	5.04	3.45	8.63	8.79	7.48	6.53	0.87
$''$	$''$	8.75	13.75	14.02	9.56	10.39	1.09
4.94×10^8	4.89	3.45	14.91	15.20	11.12	11.20	1.01
$''$	$''$	8.75	23.75	24.21	15.36	17.84	1.16
1.62×10^9	6.40	8.85	13.09	13.34	9.80	9.77	1.00
2.40×10^9	6.18	8.85	10.79	10.99	6.14	7.99	1.30
2.05×10^9	6.19	8.85	11.67	11.89	7.81	8.64	1.11
1.59×10^9	6.25	8.85	13.26	13.50	9.37	9.83	1.05
1.62×10^9	6.26	8.85	13.14	13.80	9.02	9.74	1.08
1.10×10^9	6.51	8.85	15.88	16.30	10.37	11.75	1.13
8.22×10^8	6.59	8.85	18.39	18.94	10.63	13.71	1.29
6.03×10^8	6.67	8.85	21.48	21.89	13.16	16.07	1.22
3.33×10^8	6.76	8.85	28.82	29.37	20.56	21.61	1.05

Table 1: Tabulated values for the observed arrival time and the estimates of arrival time of the LEE for all experiments for which the secondary instability is not present. The meanings of the estimates are described in the text.

flow is steady. Brooker *et al.* [9] noted that in fact there may be some effect, and developed a form of the stability equations which were similar to the parabolised stability equations (PSE) usually applied to slowly spatially varying flows, but taking account of the slow time variation. These collapse on to the usual Orr-Sommerfeld equations when the time varying terms are dropped.

Although there is some influence of the slow time dependence, the effect diminishes after relatively short time scales. As shown below, it is difficult to identify from the experimental results the actual time when this effect becomes visible and the additional accuracy obtained from solving the more difficult PSE is not warranted, in this paper at least. Consequently, the stationary form of the stability equations is relevant here.

The procedure for solution of the stationary form has been discussed above. The amplification spectrum for the case shown in figure 2 is shown in figure 7 below (Armfield, private communication). By interpolating between the curves for $t = 7$ s and $t = 8$ s, the boundary layer becomes unstable at $t = 7.5$ s, at a wave number $\alpha = 150$ m $^{-1}$. Similar spectra could be drawn for the other experiments, but are not shown here. In figure 7, the times are after initiation of the heating.

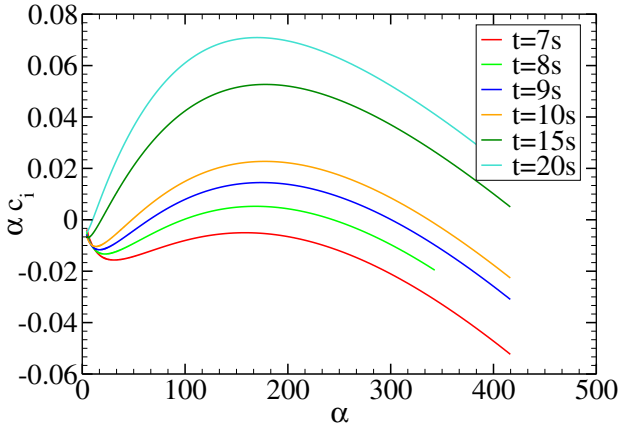

Figure 7: The amplification αc_i (s^{-1}) as a function of wave number α (m^{-1}) for the times after initiation of heating shown on the figure.

In principle therefore, for a given experiment, the one dimensional thermal boundary layer will become unstable along its full length at the time (and wavenumber) for which the amplification first becomes positive, denoted t_C. The LEE model of boundary layer development described above is therefore modified by the presence of this additional instability, as follows. Noting that t_C is fixed for a given set of parameter values, at any particular position along the layer, for $t < t_C$ and $t < t_{CR}$, the boundary layer will grow following the standard one dimensional form given by equation (7). If $t_C < t_{CR}$, the one dimensional form will continue, but will be weakly modified by the perturbation for the period $t_C < t < t_{CR}$. For $t > t_{CR}$, the LEE effect has arrived and the following oscillations are present, though these may also be modified by the instabilities already present. If, at a given location, $t_{CR} < t_C$, the LEE arrives before the secondary instability occurs and the development is as described as earlier. Note that there will always be some period for which $t < t_C$, and that for some region close to the upstream end of the wall, $t_{CR} < t_C$. On the other hand, as the downstream position increases, t_{CR} becomes increasingly larger than t_C. Further, the peak amplification rates for the first 20 s are small (see figure 7). Consequently, for locations near the upstream end, it is expected that the weak perturbations introduced by the experiments will have had insufficient time to grow to significance before the LEE arrives. On the other hand, at larger downstream distances, there is a significant time

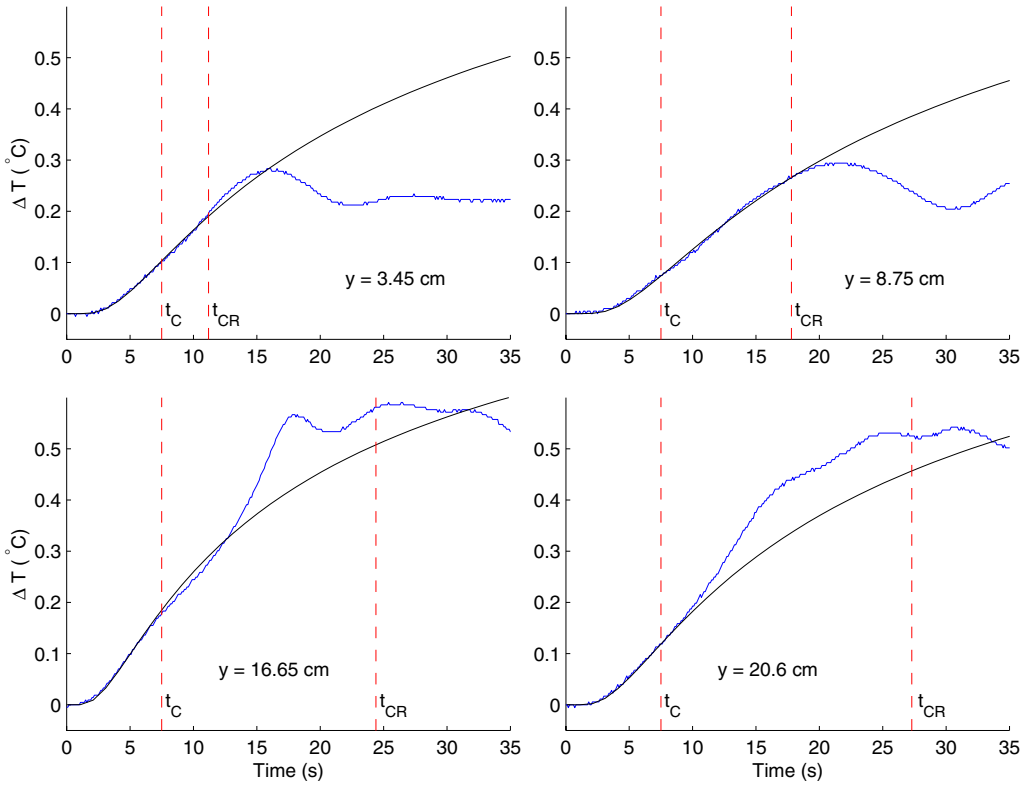

Figure 8: The first 35 s of the time series of each of the four thermistors located in the boundary layer, at the locations identified on the figures. Also shown are the one dimensional solutions, and the times t_C and t_{CR}.

separation between t_C and t_{CR}, and there may be signidficant growth of the perturbations before the arrival of the LEE.

This effect is demonstrated in figure 8. Here, the four time series from the experiment discussed above are again shown. In this case, only the first 35 s is shown, for each time series individually. On each time series figure, the times for t_C and t_{CR} are shown as broken vertical lines, and the one dimensional solution given by equation (7) is overlain.

The first panel, for the time series taken from a thermistor located 3.45 cm above the leading edge, shows that for the relatively short period betwen t_C and t_{CR}, there is virtually no deviation from the one dimensional solution. Although there is a period for which the secondary instability is active, evidently the amplification is insufficient to cause a visible deviation. Once t_{CR} is reached, the LEE arrives, and the deviation from the LEE becomes evident. A similar conclusion may be reached for the second thermistor, located at $y = 8.75$ cm. The third and fourth time series, from thermistors located at 16.65 cm and 20.65 cm however show a significant deviation from the one dimensional solution almost immediately t_C is reached, with highly amplified distrubances evident in the time immediately prior to t_{CR}, consistent with the increased time available for amplification. Time series from other experiments show similar behaviour,and are not shown here.

Conclusions

The times determined by experiment for the arrival of the LEE on the vertical heated boundary layer have been shown to be well predicted by the times obtained by integrating the maximum phase velocity of the waves generated at the leading edge by the perturbation caused by the start up of the flow. These results lend strong support to the model of [4] for the transition from one- to two-dimensional flow occurring at the time given by the passage of the fastest travelling wave originating at the leading edge.

A second instability on the boundary layer which occurs simultaneously along the one dimensional layer has also been identified. At downstream locations, this instability may occur before the arrival of the LEE, and therefore provides an alternative deviation from the one dimensional solution. The time series from one particular experiment are shown to demonstrate the effects of this instability. Although not conclusive, the data indicate that the magnitude of the perturbations increases with downstream position, consistent with the principle that, since the time taken for the LEE to arrive is longer, the perturbations have a longer period to amplify and therefore become more easily visible.

Acknowledgements

Useful discussions with Chengwang Lei, Gary Brassington and Mark Lee are acknowledged. Mark Lee has also provided expert assistance in the laboratory and in data analysis. Steve Armfield provided the stability analysis included in this paper, and as always has been a valuable source of ideas and information.

References

[1] Batchelor, G.K., Heat Transfer by Free Convection across a Closed Cavity between Vertical Boundaries at Different Temperatures. *Q. Appl. Maths*, **12**, 1954, 209–223.

[2] Patterson, J. C. and Imberger, J. 1980 Unsteady natural convection in a cavity. *J. Fluid Mech.* **100**, 1980, 65–86.

[3] Patterson, J.C. and Armfield, S.W., Transient features of natural convection in a cavity. *J. Fluid Mech.* **219**, 1990, 469 – 497.

[4] Armfield, S.W. and Patterson, J.C. Wave properties of natural convection boundary layers. *J. Fluid Mech.* **239**, 1992, 195–211.

[5] Schladow, S.G., Oscillatory motion in a side heated cavity. *J. Fluid Mech.* **213**, 1990, 589–610.

[6] Schöpf, W. and Patterson, J.C., Natural convection in a side heated cavity: visualization of the initial flow features. *J. Fluid Mech.* **295**, 1995, 357–379.

[7] Schöpf, W. and Patterson, J.C., 1996 Visualisation of natural convection in a side-heated cavity: transition to the final steady state. *Intl J. Heat and Mass Transfer* **39**, 1996, 3497–3510.

[8] Brooker, A.M.H., Patterson, J.C. and Armfield, S.W., Non parallel stability analysis of the vertical boundary layer in a differentially heated cavity. *J. Fluid Mech.* **352**, 1997, 265-281.

[9] Brooker, A.M.H., Patterson, J.C., Graham, T. and Schöpf, W. Convective instability in a time dependent buoyancy driven boundary layer. *Intl J. Heat Mass Transfer* **43**, 2000, 297–310.

[10] Daniels, P.G. and Patterson, J.C. On the long-wave instability of natural convection boundary layers. *J. Fluid Mech.* **335**, 1997, 57–73.

[11] Daniels, P.G. and Patterson, J.C. On the short-wave instability of natural convection boundary layers. *Proc. R. Soc. Lond. A* **457**, 2001, 519–538.

[12] Gebhart, B. and Mahajan, R.L.Instability and transition in buoyancy induced flows. *Adv. Appl. Mech.* **22**, 1982, 231–315.

[13] Joshi, Y. and Gebhart, B. Transition of vertical natural convection flows in water. *J. Fluid Mech.* **179**,1987, 407–438.

[14] Gebhart, B., Jaluria, Y., Mahajan, R.L. and Sammakia, B. 1988 *Buoyancy induced flow and transport.* Hemisphere, New York.

[15] Siegel, R., Transient Free Convection from a Vertical Flat Plate. *Trans. ASME J Heat Transfer*, **80**, 1958, 347–359.

[16] Illingworth, C.R., Unsteady Laminar Flow of a Gas Near an Infinite Flat Plate. *Proc. Camb. Phil. Soc.*, **46**, 1950, 603–613.

[17] Goldstein, R.J. and Briggs, D.G., Transient Free Convection about Vertical Plates and Circular Cylinders. *Trans. ASME J. Heat Transfer*, **86**,1964, 490–500.

[18] Ostrach, S., Laminar Flows with Body Forces, in *Theory of Laminar Flows* ed F.K. Moore, Princeton University Press, 1964, 528–718.

[19] Brown, S.N. and Riley, N. Flow past a suddenly heated vertical plate. *J. Fluid Mech.* **59**, 1973, 225-237.

[20] Graham, T. and Patterson, J.C. Unsteady natural convection adjacent to a semi-infinite vertical plate: an experimental study. in *Proc. ISTP-9*, editors S.H. Winoto, Y.T. Chew and N.E. Wijeysundera, Pacific Centre of Thermal-Fluids Engineering. 1996 Vol II, pp927-932.

[21] Patterson, J.C., Graham, T., Schöpf, W. and Armfield, S.W. Boundary Layer Development on a Semi-infinite Suddenly Heated Vertical Plate. *J. Fluid Mech.*2001, (in press)

[22] Le Quere. Accurate Solutions to the Square Thermally Driven Cavity at High Rayleigh Numbers. *Computers Fluids* **20**, 1991, 29–41.

[23] Paolucci, S. and Chenoweth, D.R. Transition to Chaos in a Differentially Heated Cavity. *J. Fluid Mech* **201**, 1989, 379–401.